Application Note
Reed Switch Replacement with TI's Hall-effect and Linear 3D Hall-effect Sensors

TEXAS INSTRUMENTS

Brian Dempsey

ABSTRACT

In today's world, the intersection of IoT and home security have created a wide variety of home security solutions. One of the front-runners is the door and window sensor, which typically utilizes a Reed switch to detect open and close events for a specific location. This report explores two alternative sensing solutions to Reed switches – Hall-effect switches and linear 3D Hall-effect sensors – and how they can help improve your design. This document delivers side-by-side performance comparisons of a Reed switch, the DRV5032, which is a low power Hall-effect switch, and the TMAG5170, which is a linear 3D Hall-effect sensor that provides 3-axis linear output for improved tamper detection functionality, added mechanical flexibility, and improvement over the binary output of Reed switches and Hall-effect switches. This application note also evaluates the performance and tampering susceptibility of all three types of devices and shows the strengths and weaknesses of each accordingly.

Table of Contents

List of Figures

Trademarks

All trademarks are the property of their respective owners.

1 Introduction

Door and window sensors make up the backbone of any home security system and are specifically intended to monitor which doors and windows are opened and closed within a home or office. These devices are mostly battery operated and communicate with a main security system hub with information as to whether a door or window is open/closed. If an event occurs in which a door or window gets opened or breached when the alarm is on, the sensor sends an alert signal to the main control panel and immediately triggers the main alarm.

If we dive deeper into the internal workings of the door/window sensor, there is one device that is clearly integral to the functionality of this device, a ferromagnetic sensitive device. This can be a simple Reed switch or a Hall Effect sensor, but which is better for your design and why?

The subsequent sections of this article provide an overview of the common Reed Switch, the DRV5032, and the TMAG5170 in addition to a test/result based comparison with respect to performance and tamper susceptibility.

2 Reed Switch Overview

The Reed switch is probably one of the most prevalent components found in today's door and or window sensor. The switch is essentially a glass tube filled with inert gas with two small blades comprised of some ferromagnetic material. These devices can come in N.O. (normally open) and N.C. (normally closed) configurations, but for much of the building security industry, the normally open contacts are the most popular choice. A common Reed switch is shown in Figure 2-1 along with a simple circuit that leverages the switch in a manner suitable for our application.

Figure 2-1. Reed Switch and Simple Circuit

There are also post-production problems that occur with the use of a Reed switch that can be of concern. One major concern can be the limited lifetime of the Reed Switch. Because of the mechanical nature of this device, the lifetime of the device is limited due to natural wear and tear of the physical switch.

Another issue can be power consumption on the Reed switches depending on the peripheral circuitry used. If the switch is pulled up to a source voltage when the switch is open, there will be a current associated with this pull-up network. In other configurations, there will be a small current through a pull-down or pull-up resistor when the switch is closed. There are however configurations that can be used to minimize this consumption. These are listed below:

- It can be a sampling of the pull-up resistor. This means the voltage the pull-up is tied up to is controllable. Typically, an IO pin turned on for a few µs while another IO checks the voltage across the Reed switch.
- It can also be a more complex circuit using capacitor and other circuitry to avoid constant current consumption.
- It can also be a 3 terminal Reed switch. In that case the power consumption can be 0.

3 Hall Effect Sensor Overview

Hall effect sensors, unlike Reed switches, are IC devices that can also be used to detect magnetic fields. Some of the Hall Effect sensors Texas Instruments offers, such as the TMAG5273 and the TMAG5170, can even provide 3D spacial magnetic sensing with a linear output. Others offer a binary output just as the Reed switch when a magnetic field is detected on a particular axis. If we were to use a DRV5032 with a 1.8 V supply voltage on VCC and 5 samples per second, the average current consumption would be only 540nA which provides a great low-power option for Reed switch replacement.

Hall Effect sensors detect the voltage difference (V) that develops on a conductor carrying an electrical current (I) in the presence of a magnetic field (B) as shown in Figure 3-1.
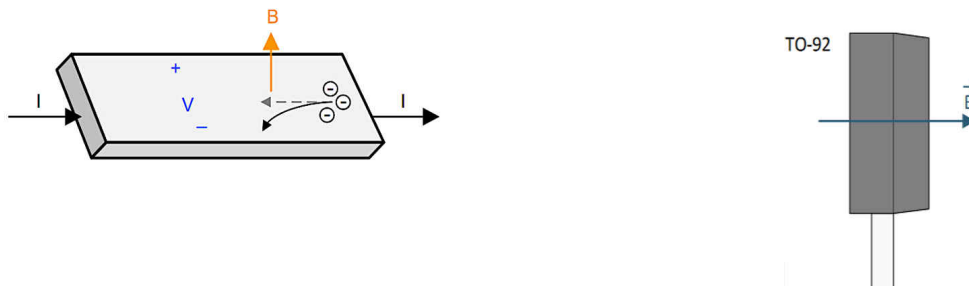

Figure 3-1. Hall Effect Sensor Working Principles and Magnetic Flux Direction

By integrating this electrophysical property into an IC, the magnetic field can be detected just as with the Reed switch. If we look at the DRV5032 schematic below, we see an example of this application leveraging a microcontroller to detect the binary output from the device. The distance of detection can be adjusted through the available magnetic threshold sensitivity variations of the product. For the testing included within this paper, we are using the omni-polar FB version of the device in a TO-92 package. More specific information on this device can be found on the DRV5032 product page on TI.com. Hall-effect switches such as the DRV5032 are suitable for applications where a simple *open* or *close* status is sufficient. This device is also very low power as well, in the nano-amp range for a 5-sample period per second. This is especially useful in battery powered applications where the design engineer must mitigate as much additional power consumption possible. An example application of the DRV5032 is shown in Figure 3-2.
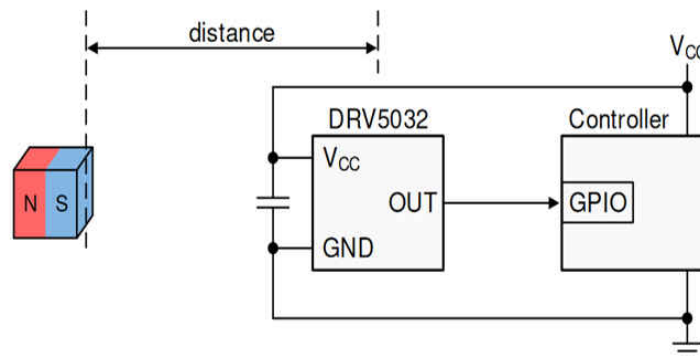

Figure 3-2. DRV5032 Application Example

Another great option for more detailed detection scenarios are linear 3D Hall-effect sensors such as the TMAG5170, which was used for testing throughout this document, and the TMAG5273. These devices are better suited for more advanced detection schemes where 3 axis detection is needed or preferred. Leveraging a 3-axis device allows for tamper detection on all three planes by using the *normal use* magnetic output as a reference point for activities. If the linear output from the device, assuming a normal idle state, is shown to vary at any point, an alert can be sent to the device owner letting them know that the sensor has detected an abnormal condition on that particular door and or window. Figure 3-3 shows an example application of the TMAG5170 with a companion host MCU.
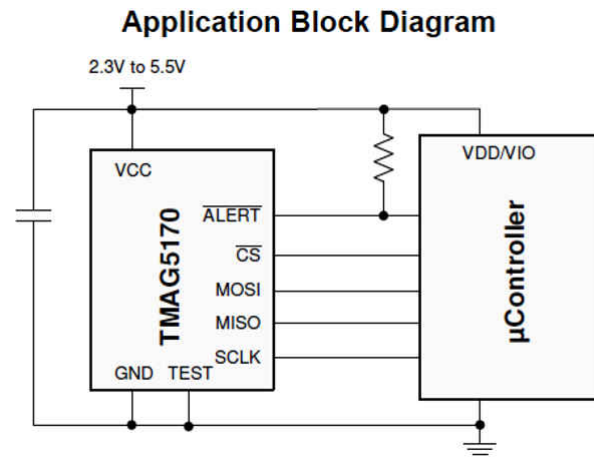
Application Block Diagram

Figure 3-3. Application Block Diagram

Linear 3D Hall-effect sensors are also a good option for sensors that require variations in mounting such as the mounting position shown in Figure 3-4. Here the door frame is raised from the door itself which creates a delta distance in both X and Y axes. While the Reed switch can still potentially work here, there are more stringent placement restrictions due to the distance and orientation of the magnet. The 3-axis TMAG devices have the ability to detect the special position of the magnet accounting for the offset added from the door frame.
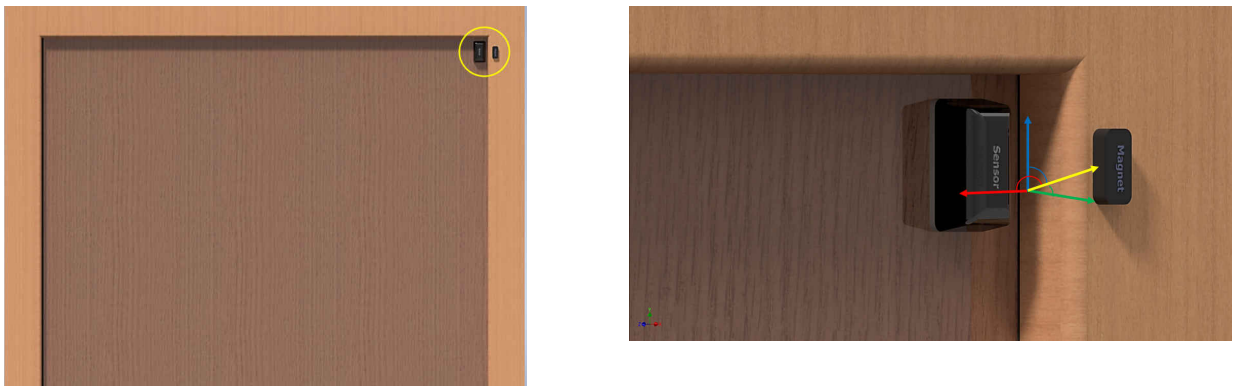

Figure 3-4. Typical Door Mounted Sensor with Raised Frame

4 Performance Comparison

This section explains the details of the test setup used for each of the devices as well as the resulting data to provide a suitable comparison of performance and repeatability in detection. For all tests explained in the ensuing sections, the same cylindrical magnet is used leveraging the same approach to the sensor/switch.

Another set of tests for these 3 devices which can be important to product designers is tamper susceptibility. In the case of door and window sensors, it goes without saying that the devices must not be susceptible to tampering through the introduction of an external magnet into the detection field of the sensor. This condition lends itself to a final set of tests to determine how efficient each device is at resisting tampering attempts. The test environment is set up per the following descriptions.

5 DRV5032 Test Setup and Results

The following sections outline the testing setup used for the DRV5032 testing as well as the respective results for each test.

5.1 DRV5032 Test Setup

The first test compares the performance of the Reed switch and the DRV5032 hall effect switch. For this test, several distances from each side of the X-axis are chosen for detection sensitivity. The Z-axis value is also varied to show sensitivity over multiple measurement nodes in the {Z,Y} plane. This test set also includes an identical testing process with variation nodes on the {X, Z} plane to show sensitivity dependency with respect to device positioning. Figure 5-1 shows the magnet approaches used for both tests.
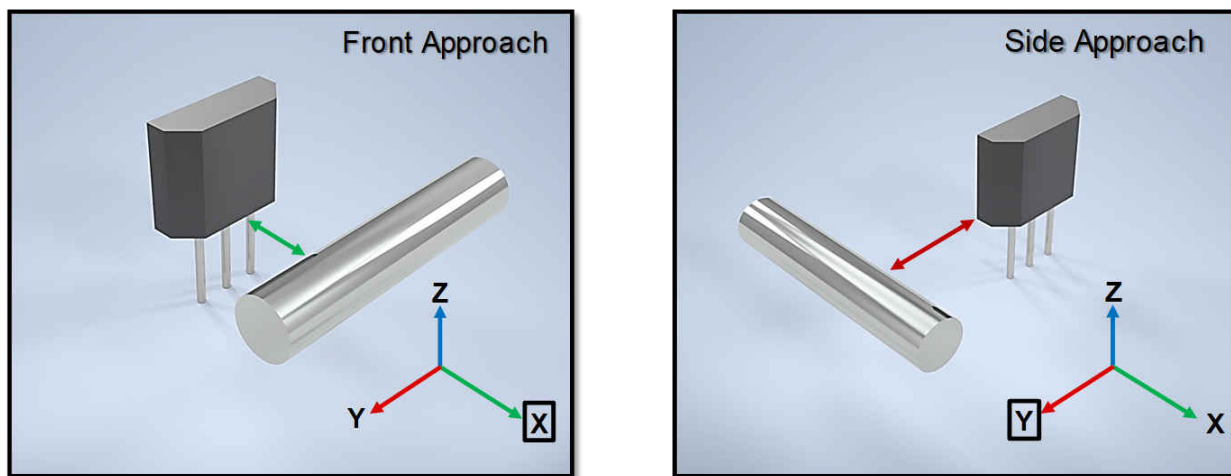

Figure 5-1. Front and Side Approach

The cylindrical magnet used in this test is magnetized through the length of the body. This creates a very low flux value at the center point of the magnet. For this reason, the center-point position along the y-axis provides no useful testing results for the DRV5032, but is added for accurate modeling purposes.

For each respective nodal coordinate (Y-axis, Z-axis), the magnet is slowly moved towards the device and the distance recorded. A standard tape measure is used for measuring the detection distance at an accuracy of 1/16th (0.0625) in. In the case of the DRV5032, the device is powered from a stable 3.3V DC power supply and populated on a small breadboard. An LED is also leveraged for visual indication of detection as well. The tape measure is only used to measure distance to the DRV5032 after the fact from a mark on a piece of masking tape and is removed during testing to negate any influence from the metal. This is shown in Figure 5-2.
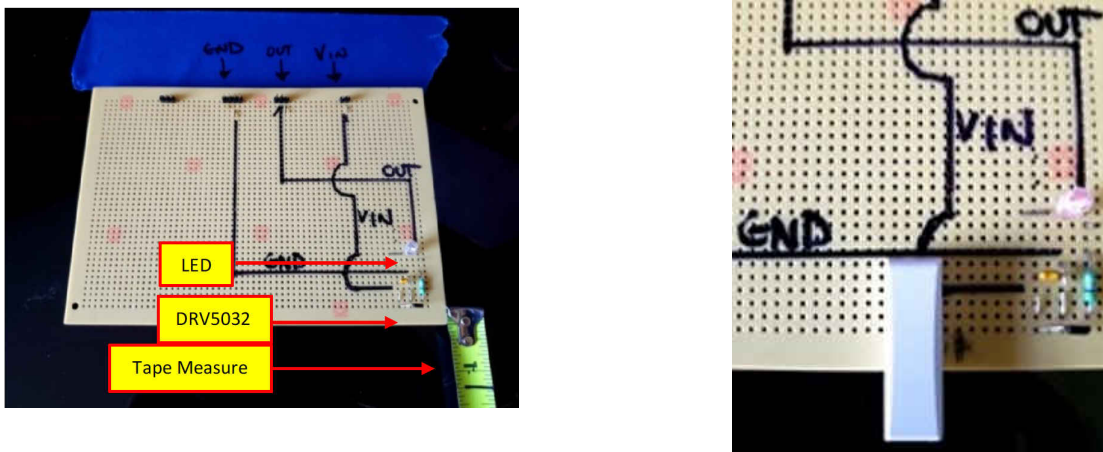
Figure 5-2. DRV5032 Test Setup

5.2 Understanding the Results

Because of the nodal testing, along with the observed detection distance on the variable axis for each specific node, a table format was used like the one shown in Figure 5-3. The sensor height remains constant throughout all testing while the change in the Y (or X in the case of the side approach) remains constant for 6 iterations of height (Z) values. The off-plane height is simply the magnets Z position minus the sensor height. Lastly, the X value in the last column is the observable detection point distance as measured during testing for each particular node.
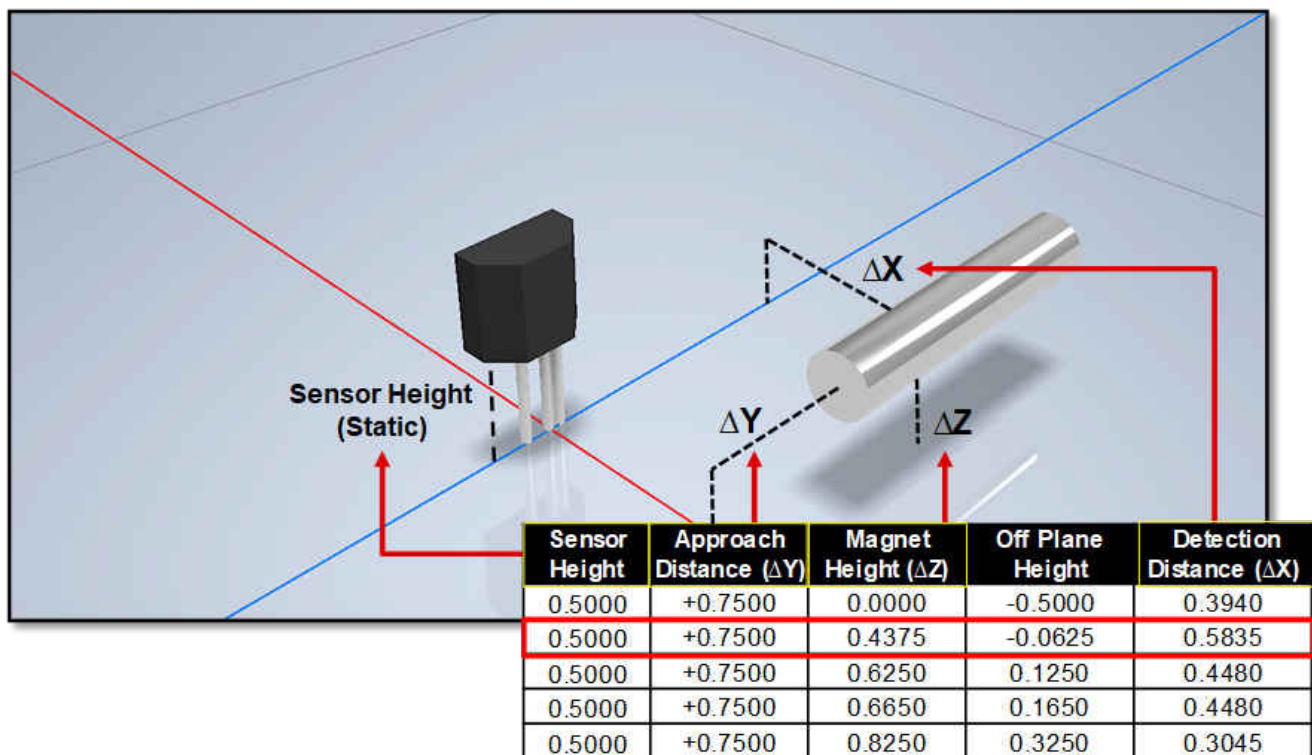

Sensor Height	Approach Distance (ΔY)	Magnet Height (ΔZ)	Off Plane Height	Detection Distance (ΔX)
0.5000	+0.7500	0.0000	-0.5000	0.3940
0.5000	+0.7500	0.4375	-0.0625	0.5835
0.5000	+0.7500	0.6250	0.1250	0.4480
0.5000	+0.7500	0.6650	0.1650	0.4480
0.5000	+0.7500	0.8250	0.3250	0.3045

Figure 5-3. Understanding the Test Results

5.3 DRV5032 Test Results

Using the test procedure described above, the test data is taken and imported into MATLAB to visualize the data for easier understanding of the performance and detection range. The ensuing sub-sections are split into front approach and side approach results and described respectively.

5.4 Front Approach Results

Figure 5-4 shows a top down three-dimensional mapping of the magnetic detection field of the DRV5032 with a top down view. From this visual, it can be seen that the maximum distance from the device that the magnet was detected was slightly less than 1 inch. As expected, there is a point in the center where the magnet was not detected, due to the magnetization characteristics of the magnet used in testing.
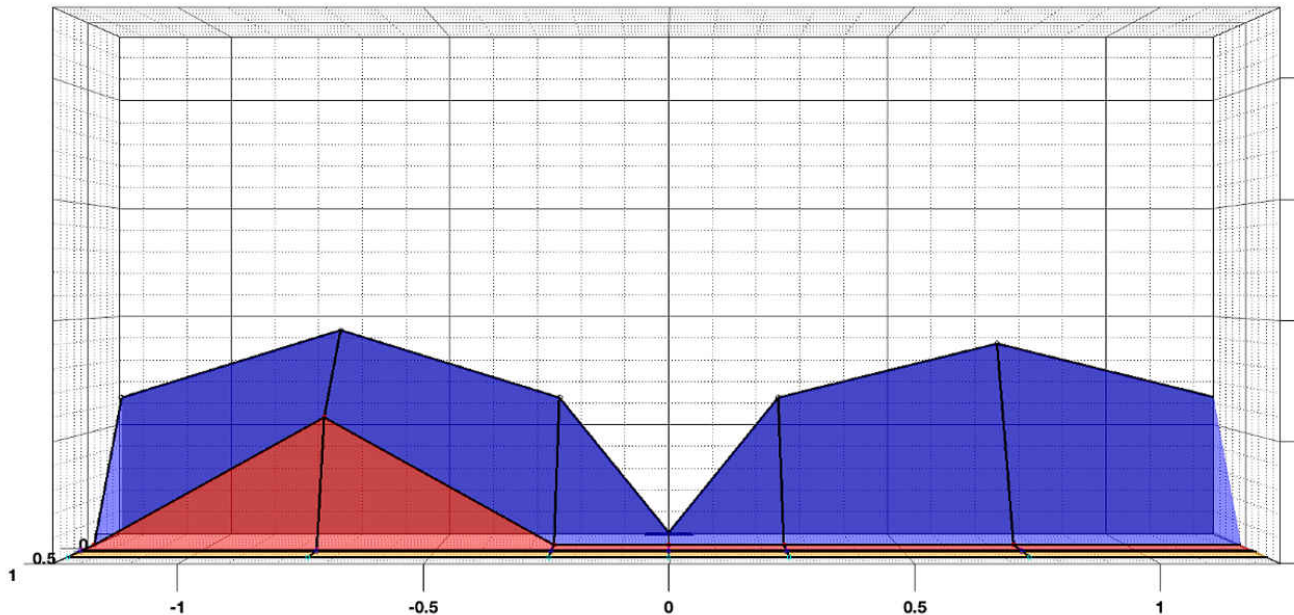
Figure 5-4. DRV5032 Front Approach Magnetic Detection Field: Top Down View

Figure 5-5 shows a side (X,Z plane) view of the detection field. This provides more details on the detection distance now adding in the sensitivity over variable height nodes. The detection height tapers sharply at approximately 0.45 inches above the DRV5032 and becomes imperceptible slightly higher than 0.6 inches on the right side (facing front of device). The variance between the left and right side can most likely be attributed to test setup limitations with respect to absolute accuracy.
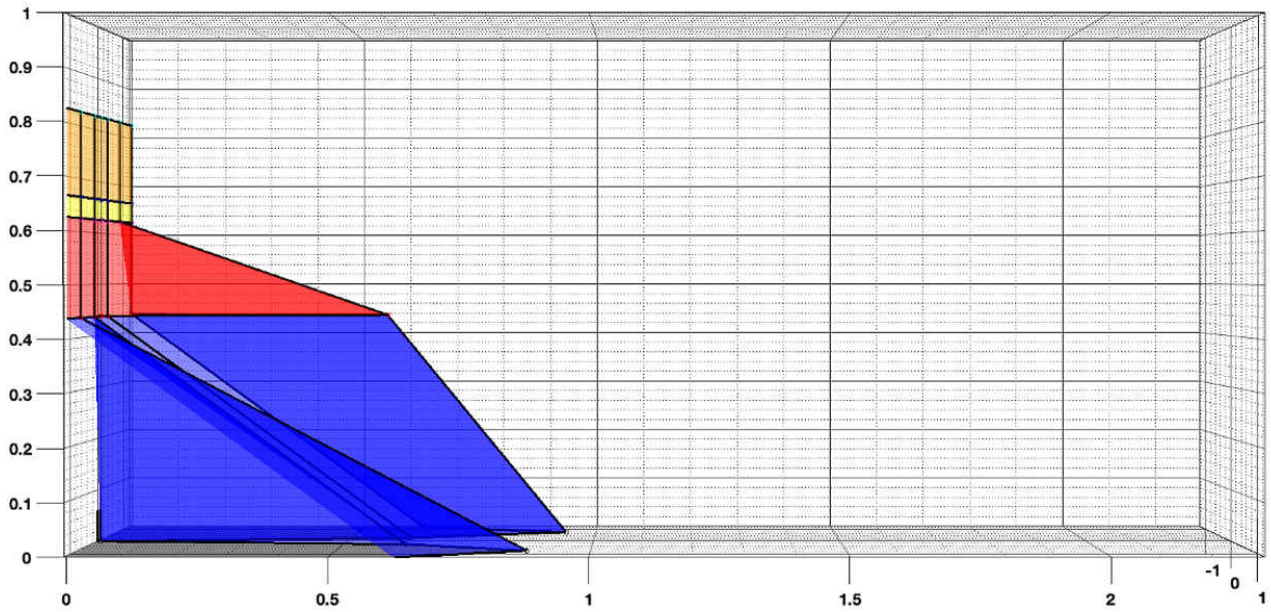
Figure 5-5. DRV5032 Front Approach Magnetic Detection Field: Side View

Finally, Figure 5-6 shows an off-axis view of the magnetic sensitivity for a big picture snapshot of the results. All of the previously mentioned key portions of the results are shown together in this plot.
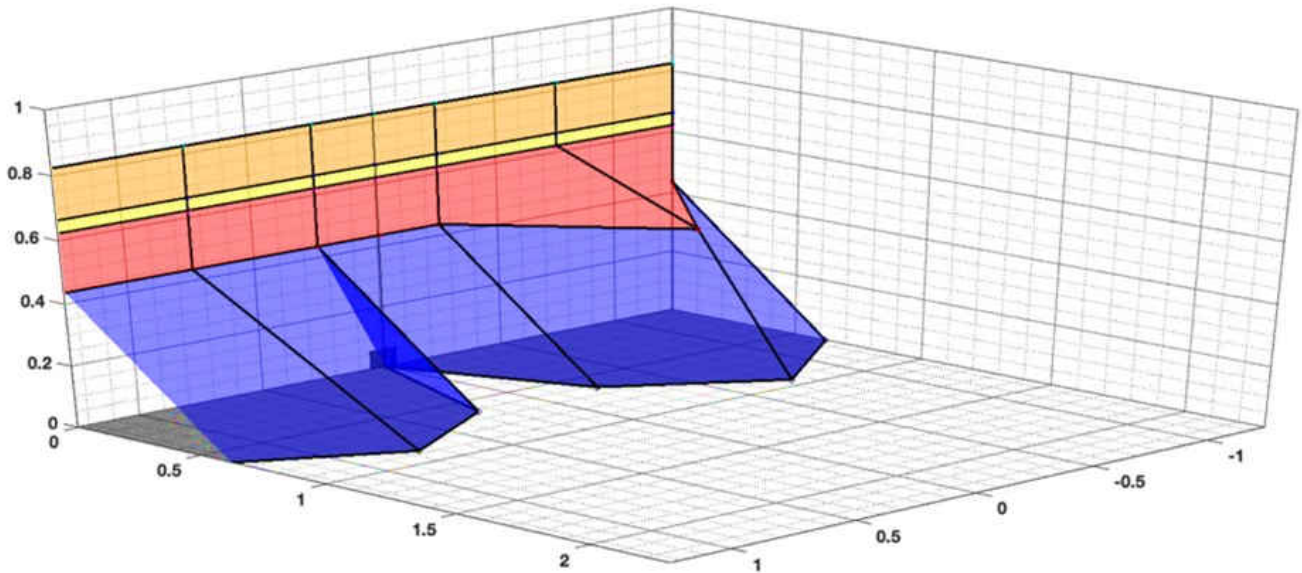

Figure 5-6. DRV5032 Front Approach Magnetic Detection Field: Off-Axis View

5.5 Side Approach

For the side approach, Figure 5-7 and Figure 5-8 show the resulting detection field using the approach shown in Figure 5-6. The detection field is very symmetrical along the X-axis with a maximum detection distance of approximately 0.75 inches at 0.25 inches in either direction off the axis, with the detection tapering from this point outwards.
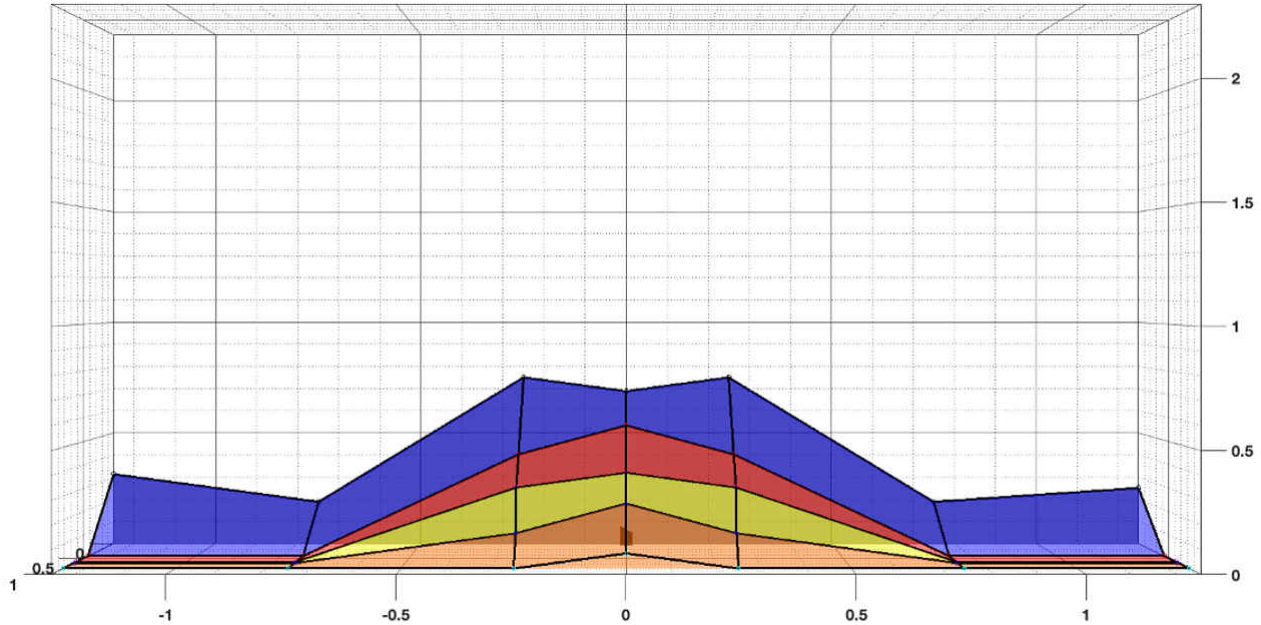
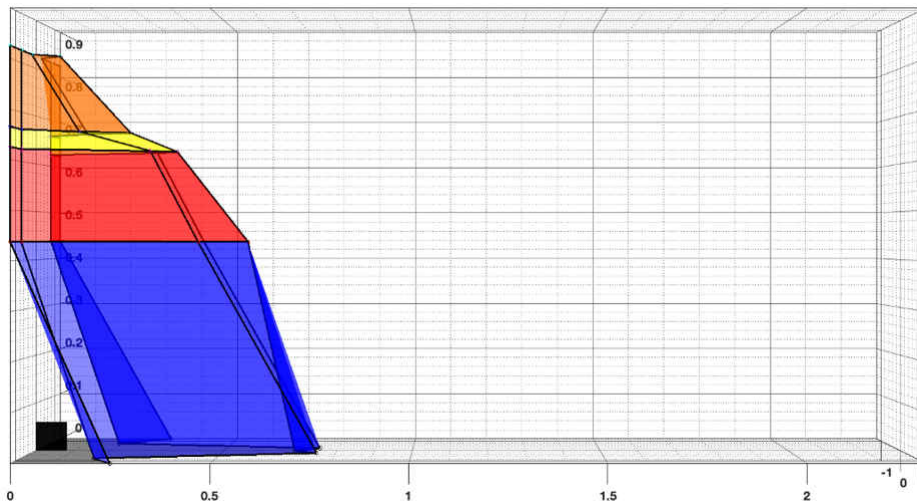**Figure 5-7. DRV5032 Side Approach Magnetic Detection Field Results: Top Down View**

Figure 5-8. DRV5032 Side Approach Magnetic Detection Field Results: Side View

Figure 5-9 shows the DRV5032 side approach field to better show the axes values and the field shape. The Z axis height sharply tapers at 0.6 inches above the device and is no longer perceptible after approximately 0.8 inches.
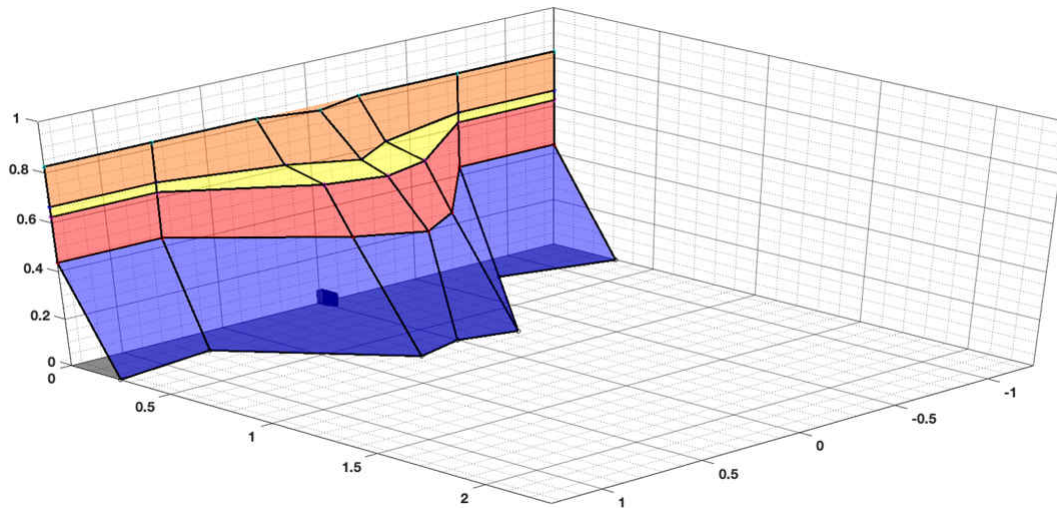
Figure 5-9. DRV5032 Side Approach Magnetic Detection Field Results: Off-Axis View

5.6 Tamper Susceptibility Testing Setup

For this test, a sliding glass door and a typical entry door is used as the main mounting point for the Reed switch and the DRV5032 tamper test. The device mounting is altered in a way to make testing more practical while imitating a typical placement for the device in a home or business. For each test, the magnet is brought closer to the door for the opposite (outside) side until the LED goes off, indicating that the sensor has detected the tamper magnet's field. Both door scenarios are shown in Figure 5-10.
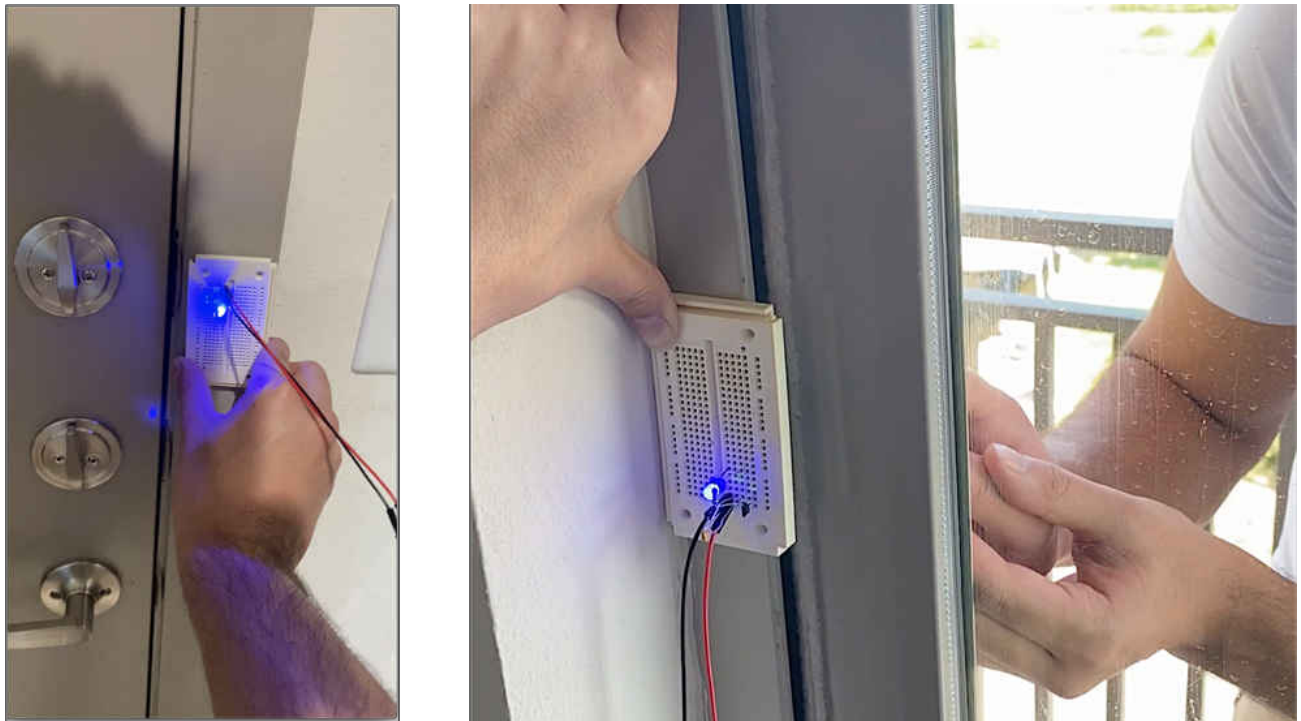
Figure 5-10. DRV5032 Tamper Test Setup

5.7 Tamper Susceptibility Test Results

- Entry door – For this test, the DRV5032 was not able to be influenced by the tamper magnet through multiple attempts. The LED remained on throughout the testing which shows an example of the resistance to tampering of the DRV5032.
- Sliding glass door – For the sliding glass door, the magnet was also slowly brought up to the device. The magnet in this case was also not able to trip the DRV5032 through the door.

6 Reed Switch Test Setup and Results

The following sections outline the testing setup used for the Reed switch testing as well as the respective results for each test.

6.1 Reed Switch Test Setup

For the Reed switch, the test setup is fundamentally the same as for the hall effect switch test. The device is already mounted on a pcb board so there is no need to implement onto a separate breadboard. Instead of using an LED for detection indication, a multimeter with a continuity function is used along with alligator clip test leads that are clamped to each respective end of the Reed switch. While no magnet is present in range of the Reed switch, there will be no continuity between the leads of the Reed switch. Once a magnet comes close enough to close the Reed switch, continuity is detected through an audible tone from the multi meter. The distance of detection can then be measured and recorded for later analysis.

6.2 Reed Switch Test Results

The ensuing subsections are analyzed based on front and aide approach of the Reed switch.

6.3 Front Approach Results

Figure 6-1 and Figure 6-2 show the resulting detection field for the Reed switch in the same views done for the DRV5032. Figure 6-1 shows the top-down view, while Figure 6-2 shows the side view. As shown, the Reed switch does have a larger detection distance over the DRV5032, but also has many more detection field variances, which can be unfavorable in security applications where these variances can give way to successful tampering attempts.
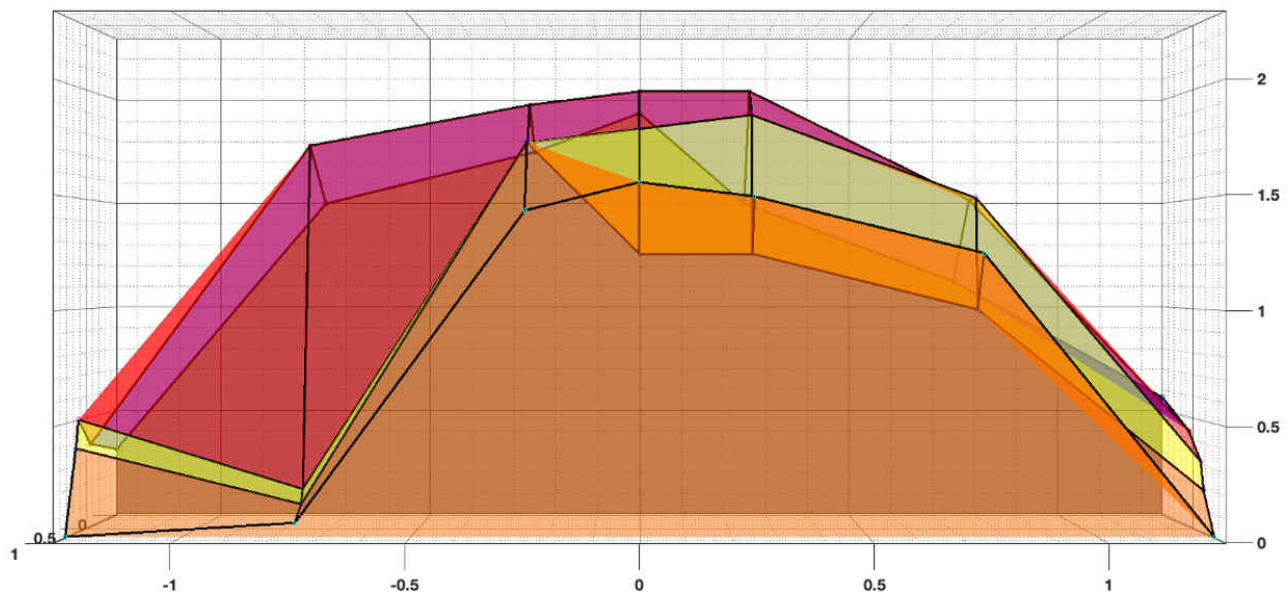

Figure 6-1. Reed Switch Front Approach Magnetic Detection Field Results: Top Down View
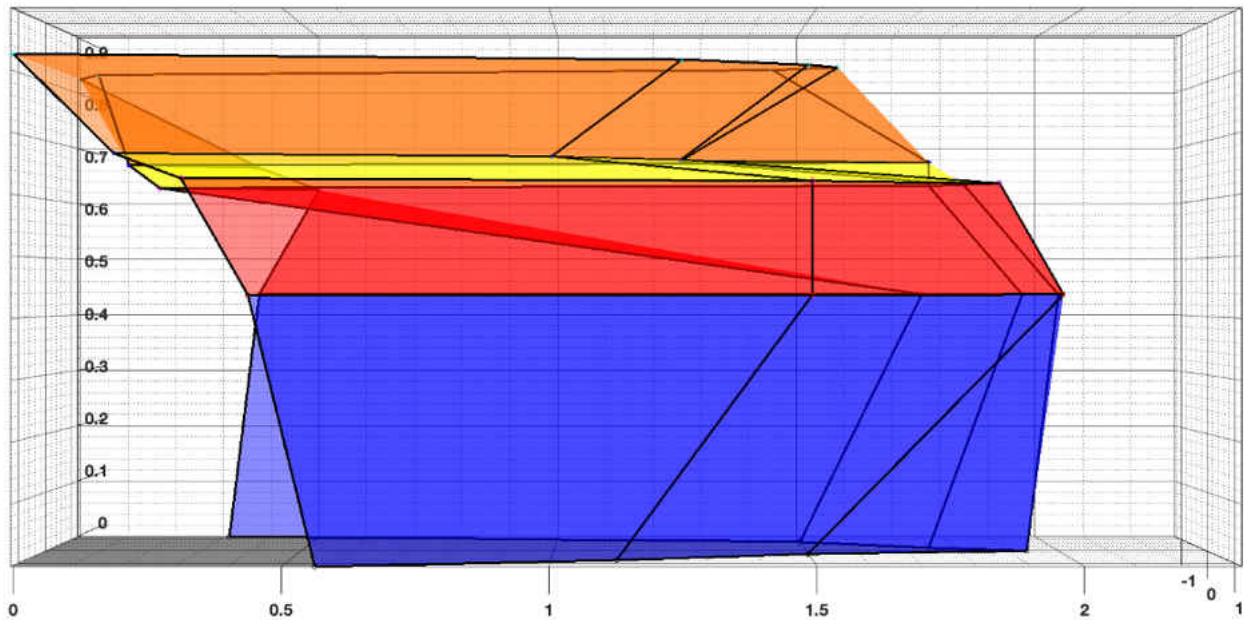
Figure 6-2. Reed Switch Front Approach Magnetic Detection Field Results: Side View

Figure 6-3 shows a rotated view to capture detection range on all 3 axes. The detection range is very spontaneous and has no observable symmetrical properties.
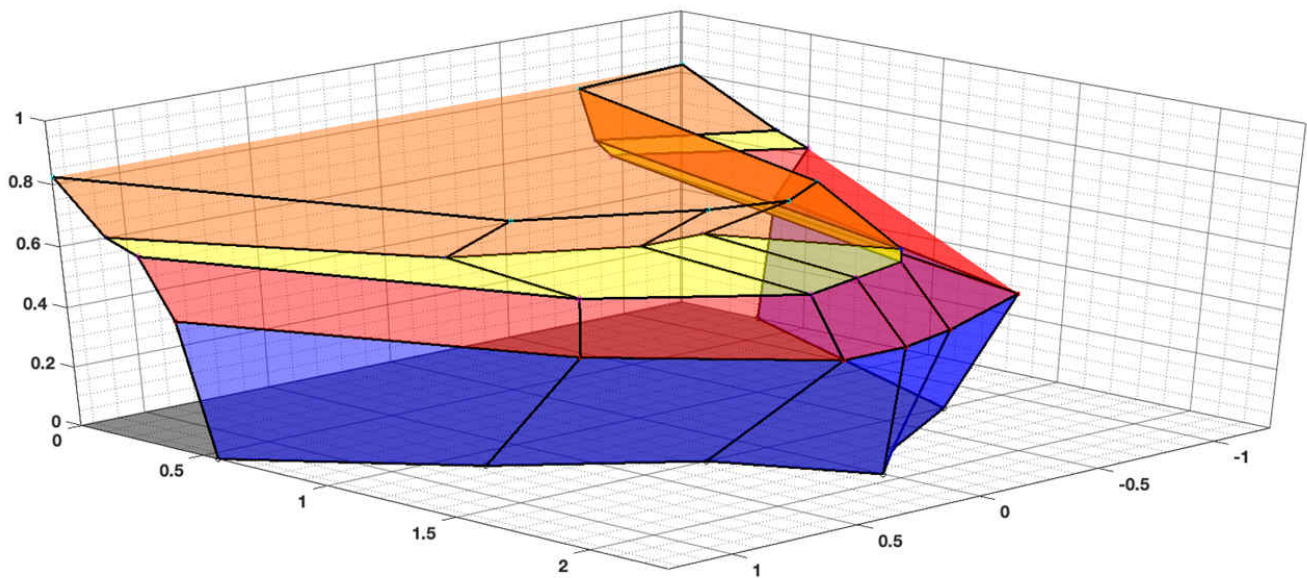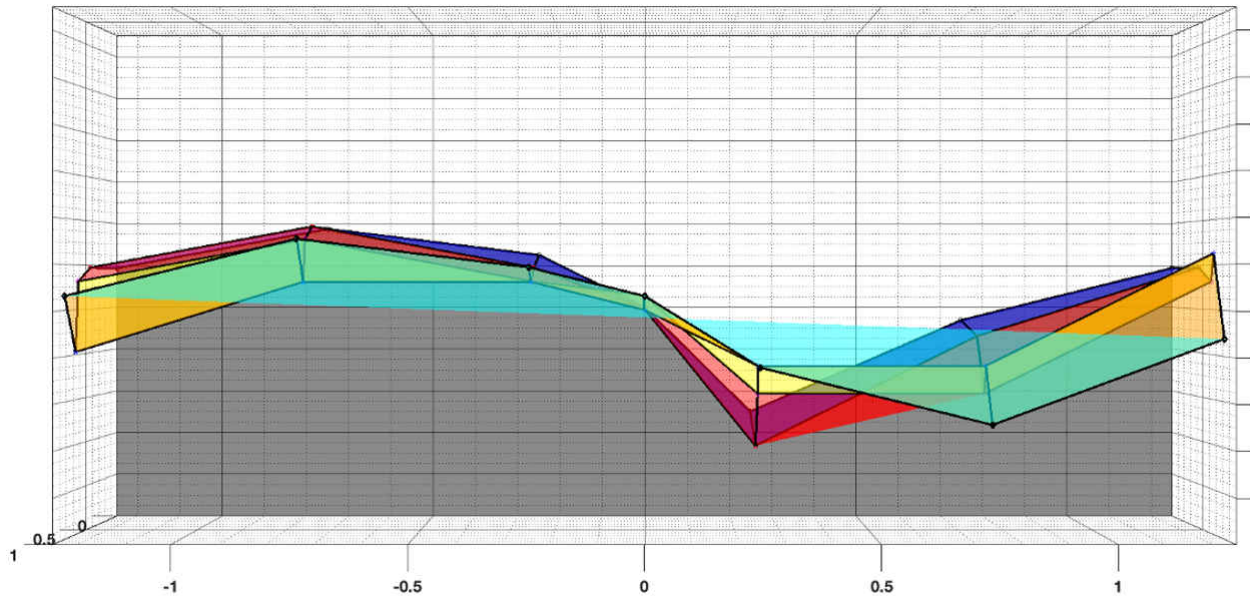

Figure 6-3. Reed Switch Front Approach Magnetic Detection Field Results: Off-Axis View

6.4 Side Approach Results

As with the DRV5032 the side approach is also done with the Reed switch to see the effect on the detection range and any blind spots. Figure 6-4 and Figure 6-5 shows these resulting magnetic detection field points for the Reed switch in both top-down approach as well as side approach. The detection field ranges from approximately 0.4 inches all the way to 1.4 inches with somewhat of a sinusoidal shape of detection along the device.

Figure 6-4. Reed Switch Side Approach Magnetic Detection Field Results: Top-down View
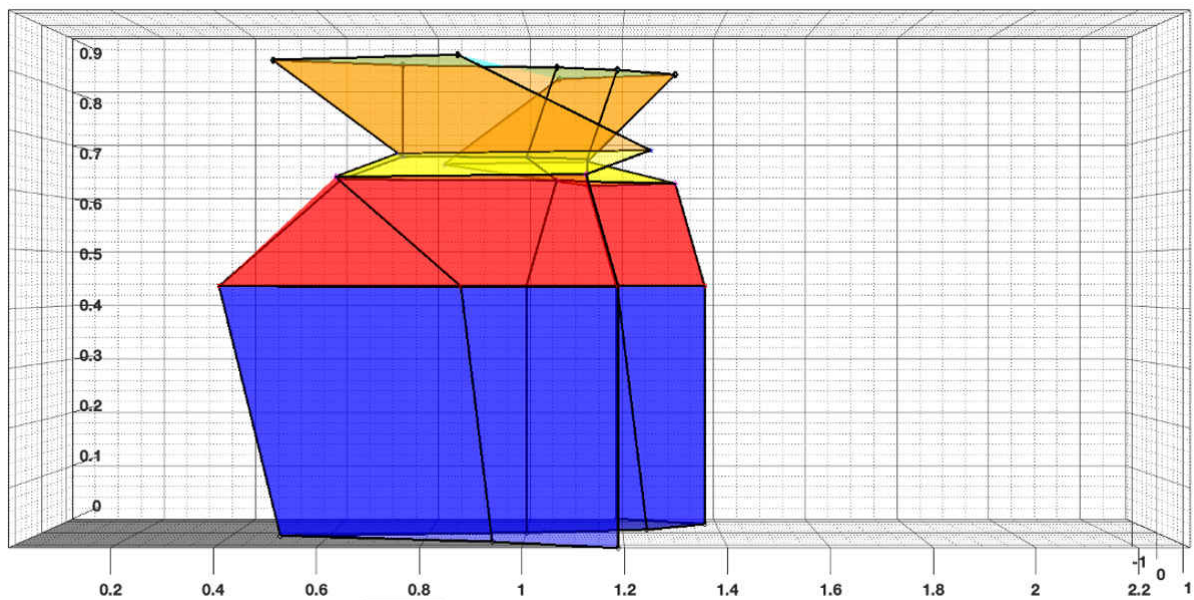
Figure 6-5. Reed Switch Side Approach Magnetic Detection Field Results: Side View

The height of detection is similar to that of the DRV5032 with a maximum Z height of approximately 0.85 inches. Figure 6-6 shows the results of the testing from an angle to show the 3 axes of data in a more comprehensible way.
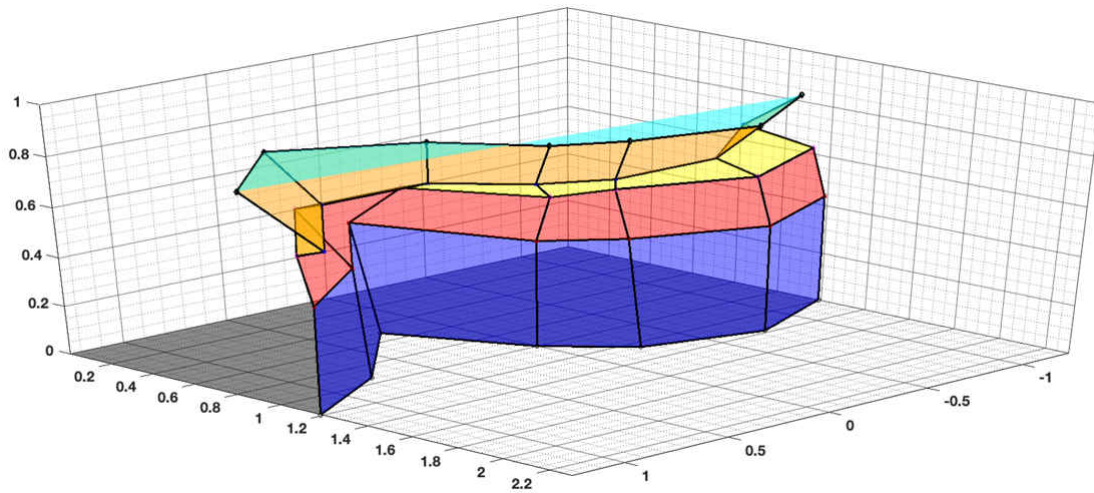
Figure 6-6. Reed Switch Side Approach Magnetic Detection Field Results: Off-Axis View

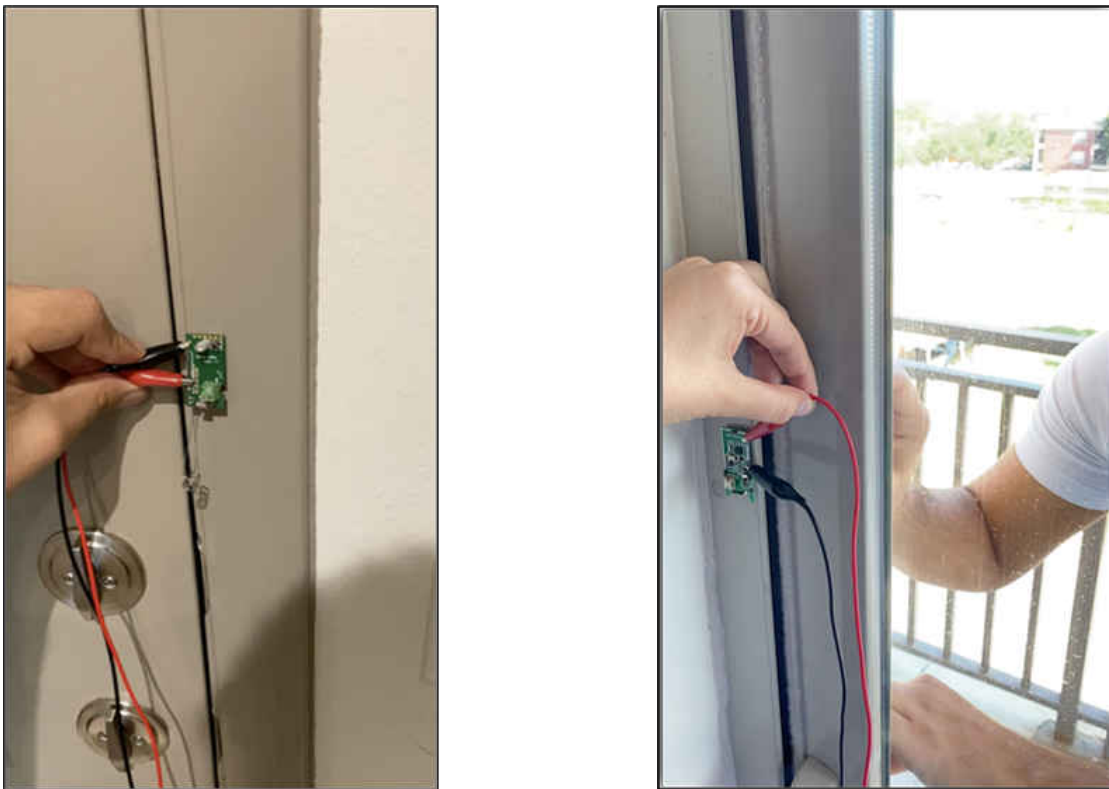## 6.5 Tamper Susceptibility Testing Setup

Figure 6-7. Reed Switch Tamper Susceptibility Testing Setup

6.6 Reed Switch Tamper Susceptibility Test Results

- Entry door – For this test, the Reed switch was influenced by the tamper magnet over multiple test trials. Audible continuity tone showed that the Reed switch contacts closed once the tamper magnet was brought close enough from the outside of the door.
- Sliding glass door – For the sliding glass door, the magnet was able to make the Reed switch contacts close from the outside of the sliding door. This indicates that the Reed switch can be rendered essentially nonfunctional from a tamper magnet in the mounting scenario shown in Figure 6-7.

7 TMAG5170 Test Setup and Results

The following section outlines the testing setup used for the TMAG5170 testing as well as the respective results for each test.

7.1 TMAG5170 Test Setup

For the TMAG5170 test setup, we leverage the TMAG5170EVM shown in Figure 7-1. This board provides all necessary connections from the TMAG device for communication with the evaluation GUI. The device is located on a protruding cantilever to isolate from the rest of the board. The measurement process in this case is the same as for the DRV5032 and Reed switch with static nodal points in the first two axes and the variance being introduced on the third.
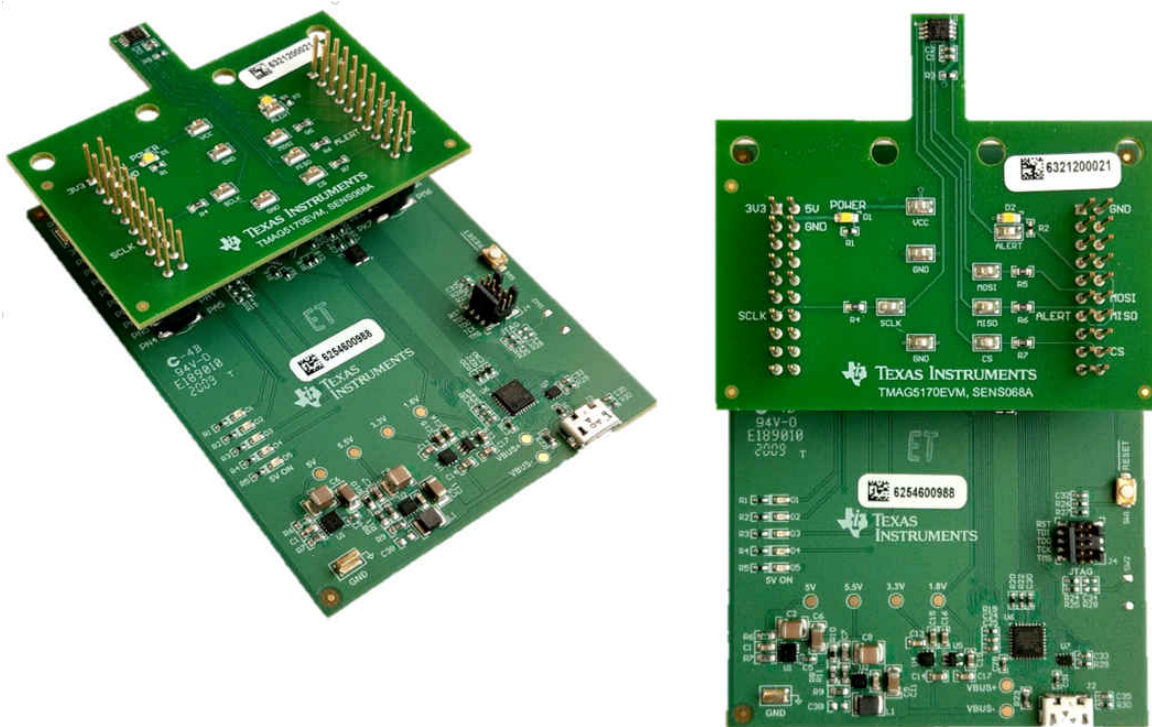

Figure 7-1. TMAG5170EVM Board

In addition to device placement, there are several parameters which can be adjusted within the GUI for different detection scenarios. For the purpose of this test, the following configuration parameters were used:

TMAG settings

- Configuration mode
- Conversions: as fast as possible
- All axes active
- 50mT range
- Magnitude calculated from X and Y axes.

Magnet: K&J Magnetics D4X0

- N42 cylindrical magnet
- Constant orientation
- Moved across grid in ¼ inch steps

The TMAG5170 testing is accomplished slightly different than the sliding door tampering method due to the nature of the device and the linear output capabilities for all three axes. In addition to bringing the magnet closer to the device on a particular axis, the device is also positioned at a 45-degree angle as well to gain an understanding of the device's response when the field is oriented on a plane rather than just an axis.
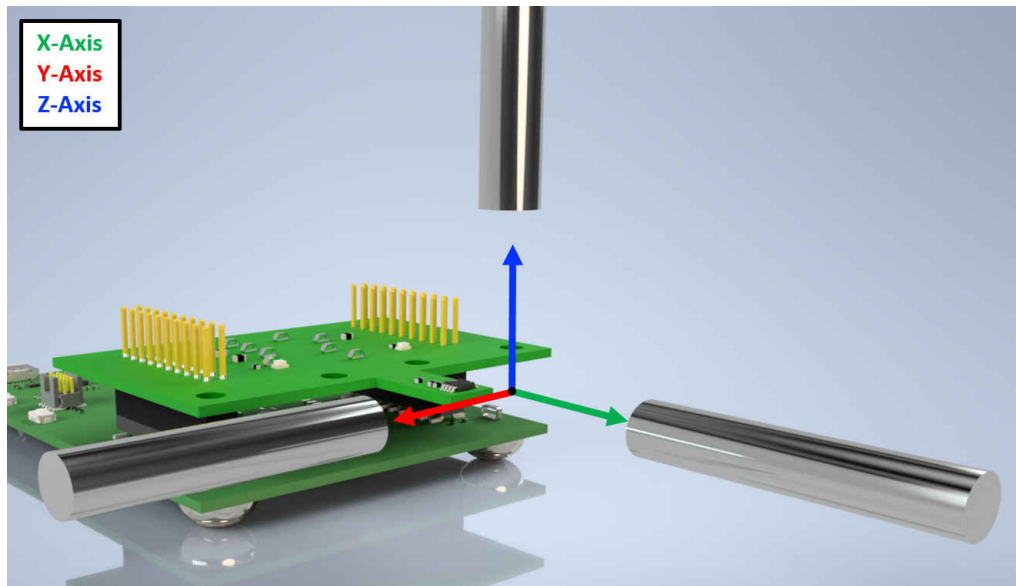
Figure 7-2. TMAG5170 Magnetic Approach Directions

This test only includes one approach data set as the other two axes would be comparatively the same as far as device response and output from the GUI. For this test, the axis of approach is the X axis shown in Figure 7-3 and Figure 7-4). The secondary test is on the X, Y plane at a 45-degree angle approach shown in Figure 7-4.

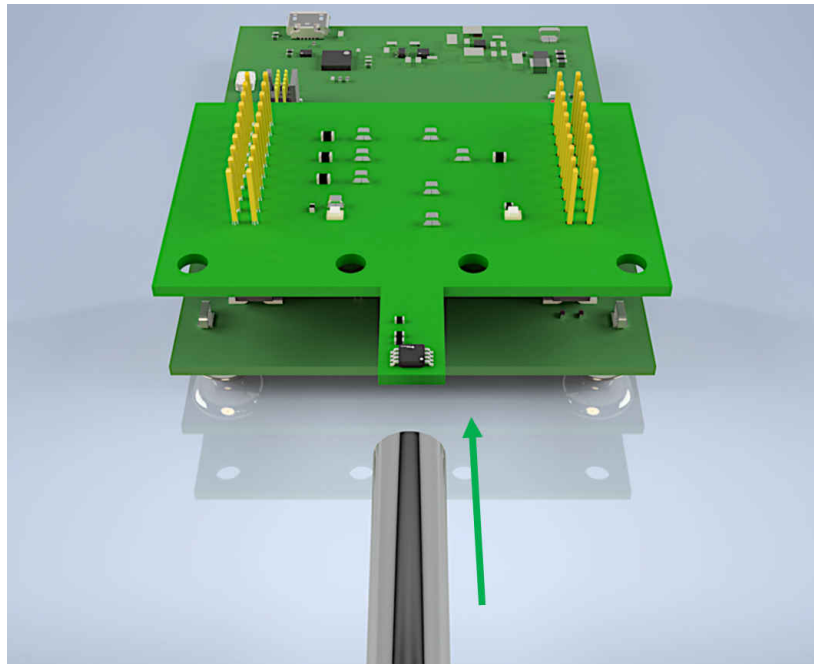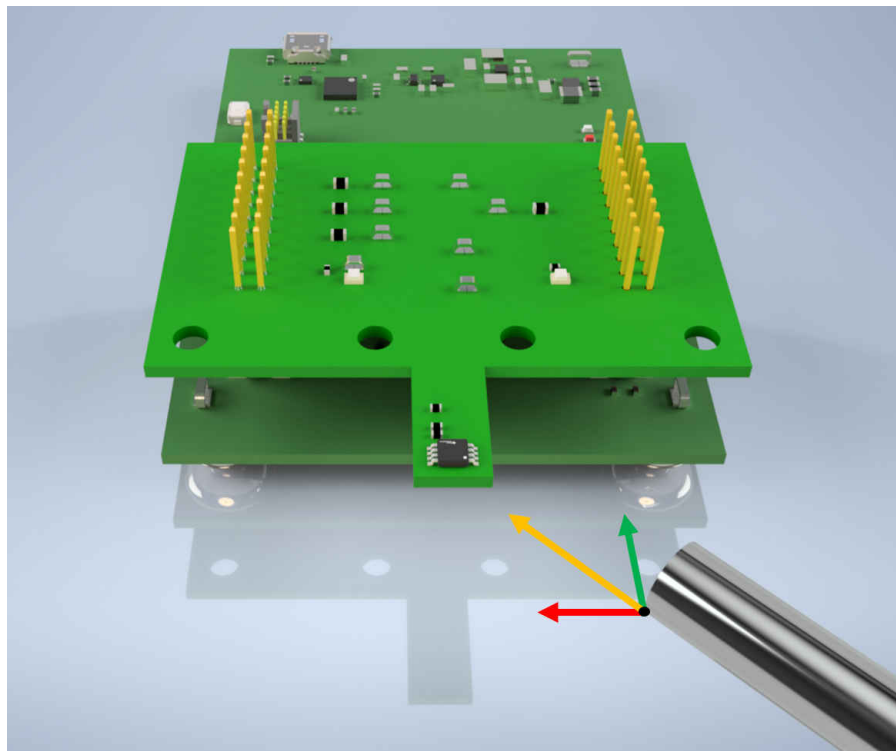**Figure 7-3. TMAG5170 X-Axis Approach**

Figure 7-4. TMAG5170 45-Degree Angle Approach

7.2 TMAG5170 Test Results

Figure 7-5 and Figure 7-6 show the resulting three-axis magnetic response of the TMAG5170 based on both approaches described previously. As shown by the output, the multiple axes remove constraints on magnetic placement allowing off axis placement to be more feasible due to the only importance being strength of field.
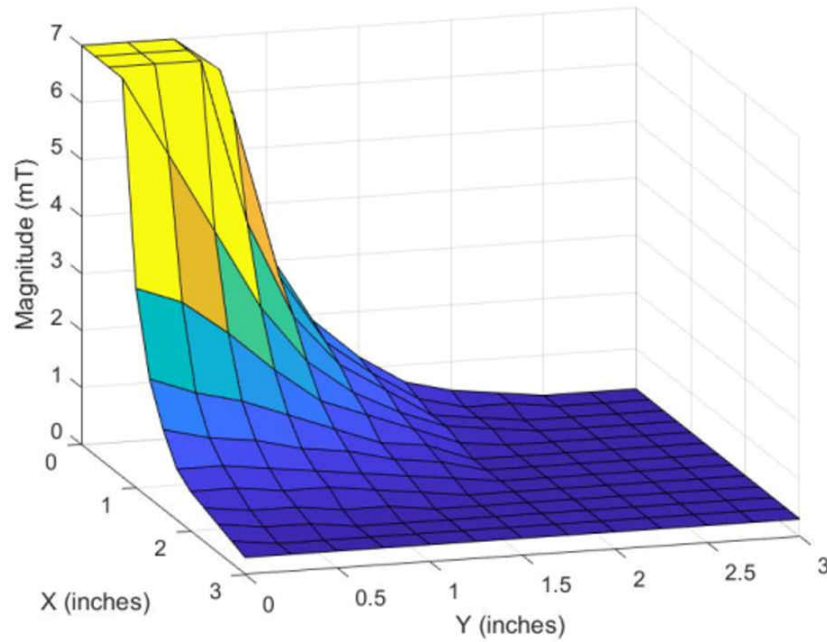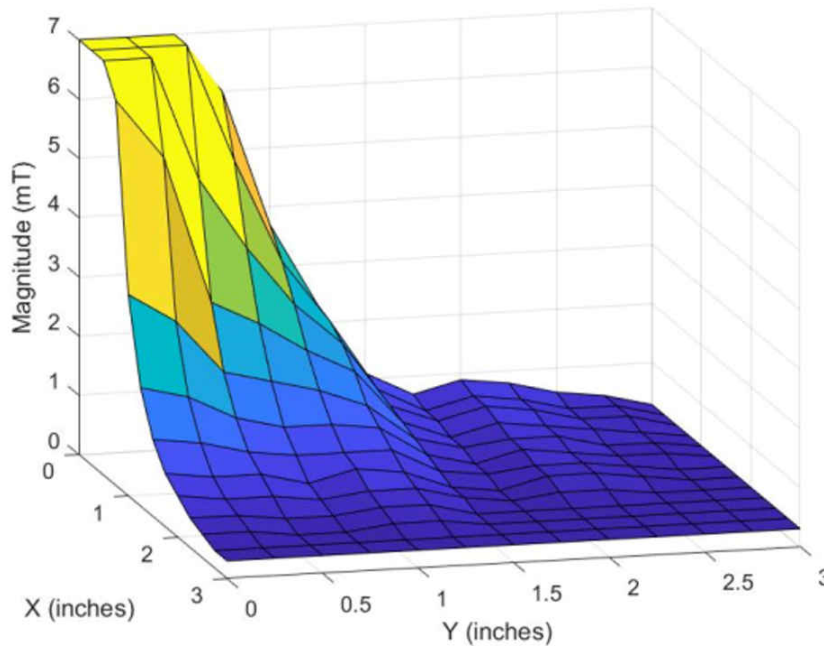

Figure 7-5. TMAG5170 On-Axis Magnetic Detection

Figure 7-6. TMAG5170 Off-Axis Magnetic Detection

7.3 TMAG5170 Tamper Susceptibility Testing Setup

As with the Reed switch and Hall-effect sensor, tamper susceptibility is also tested with the TMAG5170, in this case with 2 magnets. One is considered the genuine magnet while the other is considered the fraudulent magnet. The following outlines the setup parameters used for this test.

TMAG settings

- Configuration mode
- Conversions: 1 per second
- 8x averaging
- All axes active, 50mT range

Magnet: 2 K&J Magnetics D4X0

- N42 cylindrical magnet
- Original magnet in constant position, window/door closed
- Second magnet moved in an attempt to mimic original magnetic signature

7.4 TMAG5170 Tamper Susceptibility Test Results

The tampering was done both orthogonally as well as parallel. Figure 7-7 shows the output from the TMAG5170 GUI when the fraudulent magnet is brought within the detection field of the device. The field strength is approximately 1.75mT on the X-axis until the imposter magnet is brought closer. The introduction of the second magnet increases the field strength on both the X as well as the Y axis, indicating a tamper attempt has occurred.
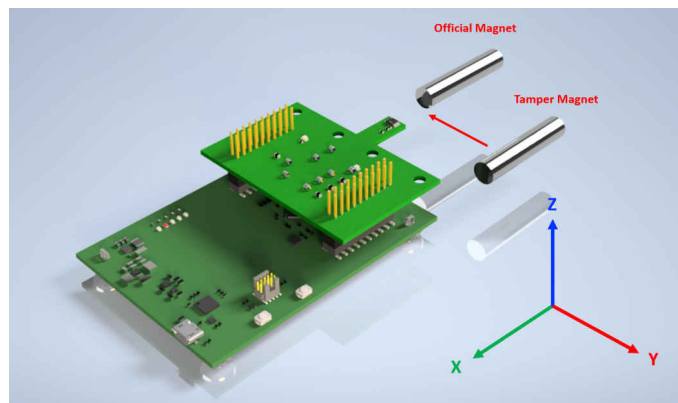
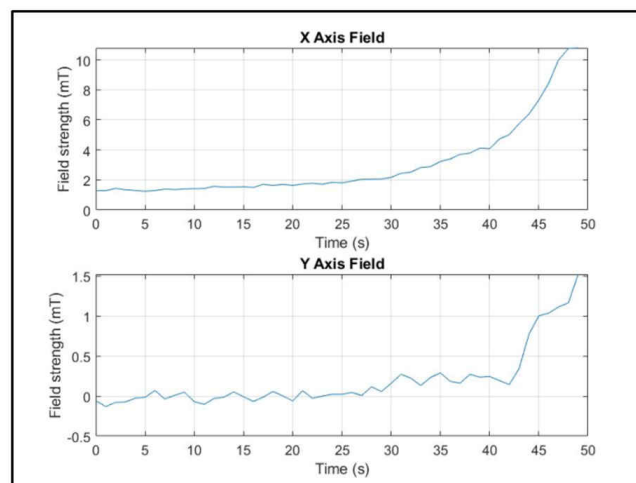**Figure 7-7. TMAG5170 Orthogonal Tamper Testing Setup**

Figure 7-8. TMAG5170 Orthogonal-Axis Magnetic Detection: Results

Again, the tampering test is done, this time parallel to the genuine magnet. Figure 7-9 shows the resulting response from the TMAG5170 when the tamper magnet is brought within detection range. Before the tamper magnet begins the approach, the X axis field strength is approximately 1.1mT. Once the tamper magnet is brought closer, the evidence of tampering attempt can be seen on the Z axis with the field strength again increasing on the X axis due to the additional magnetic field presence.
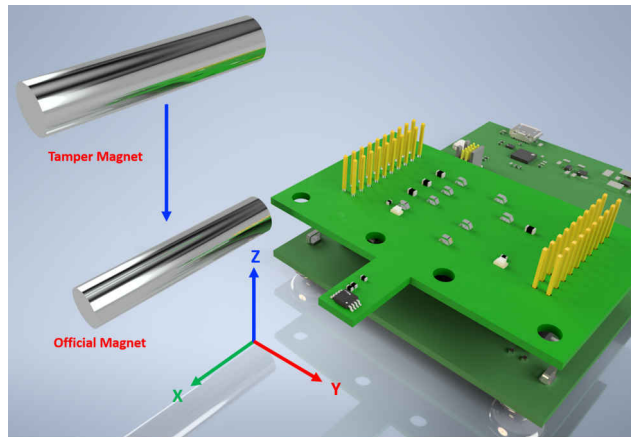

Figure 7-9. TMAG5170 Parallel Tamper Test: Setup
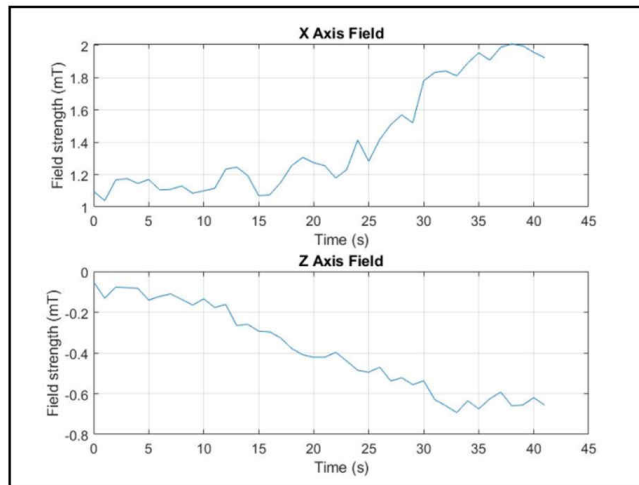
Figure 7-10. TMAG5170 Parallel Tamper Test: Results

8 Summary

Although there are several options when choosing a solution for security sensors, many factors need to be accounted for to offer the most robust solution while also offering reasonable resistance to tampering. Although the Reed switch is often the go to solution due to simplicity and relatively low initial cost, there are pitfalls associated with this device that provide erratic detection fields which can become an easy target for tampering. Low power Hall-effect switches, such as the DRV5032, can provide a nano-powered and cost competitive alternative sensing solution to Reed switches with a tighter, more symmetrical detection range. For the designer looking for added mechanical flexibility and advanced field detection capabilities, linear 3D Hall-effect sensors such as the TMAG5170 and the cost competitive TMAG5273 provide a linear response output with 3-axis detection, which can easily detect tamper attempts and stray magnetic fields. Ultimately, TI offers many robust solutions for security sensors that are both low cost and dependable. Switching from a Reed switch has never been easier!

IMPORTANT NOTICE AND DISCLAIMER